



HAL
open science

Detonation peninsula for TRF-air mixtures: assessment for the analysis of auto-ignition events in spark-ignition engines

Ahmed Guerouani, Anthony Robert, Jean-Marc Zaccardi

► **To cite this version:**

Ahmed Guerouani, Anthony Robert, Jean-Marc Zaccardi. Detonation peninsula for TRF-air mixtures: assessment for the analysis of auto-ignition events in spark-ignition engines. SAE International Journal of Engines, 2018, SAE Technical Paper 2018-01-1721. 10.1177/1468087417712160 . hal-01978654

HAL Id: hal-01978654

<https://ifp.hal.science/hal-01978654>

Submitted on 11 Jan 2019

HAL is a multi-disciplinary open access archive for the deposit and dissemination of scientific research documents, whether they are published or not. The documents may come from teaching and research institutions in France or abroad, or from public or private research centers.

L'archive ouverte pluridisciplinaire **HAL**, est destinée au dépôt et à la diffusion de documents scientifiques de niveau recherche, publiés ou non, émanant des établissements d'enseignement et de recherche français ou étrangers, des laboratoires publics ou privés.

Detonation peninsula for TRF-air mixtures: assessment for the analysis of auto-ignition events in spark-ignition engines

Abstract

Controlling abnormal auto-ignition processes in spark-ignition engines requires understanding how auto-ignition is triggered and how it propagates inside the combustion chamber. The original Zeldovich theory regarding auto-ignition propagation was further developed by Bradley and coworkers, who highlighted different modes by considering various hot spot characteristics and thermodynamic conditions around them. Dimensionless parameters (ϵ , ξ) were then proposed to classify these modes and to define a detonation peninsula for H₂-CO-air mixtures.

This article deals with numerical simulations undertaken to check the relevancy of this original detonation peninsula when considering realistic gasoline fuels. 1D calculations of auto-ignition propagation are performed using the Tabulated Kinetics for Ignition model. Chemical kinetics calculations are first carried out to build the needed look-up table for the auto-ignition delay time τ_i , and the excitation times τ_e of E10-air mixtures using a RON 95 TRF surrogate.

The dimensionless parameter ϵ is based on the hot spot radius and on the excitation time τ_e of the fuel. Previous chemical kinetics calculations confirm the impact of the fuel on this parameter as H₂-CO-air mixtures feature much longer excitation times than TRF-air mixtures. Focusing on the parameter ξ , its estimation depends on hot spots characteristics and thermodynamic conditions. The limits of the peninsula therefore vary depending on initial conditions and hot spot characteristics, that is why this paper focuses on several conditions to validate the dependency of the boundaries between the different auto-ignition modes. Hundreds of simulations are performed and due to the large amount of calculations, a specific post-processing methodology is defined to determine the auto-ignition propagation modes by automatically characterizing the coupling conditions between reaction and pressure waves. Several new detonation peninsulas are finally proposed depending on initial conditions in terms of temperature, pressure, fuel-air equivalence ratio and dilution. Limits of the detonation peninsula for TRF-air mixtures are more affected depending on each operating conditions. These new limits can finally be used to better understand abnormal auto-ignition events in spark-ignition engines.

Introduction

Two main abnormal combustions are observed in modern spark-ignition engines: knock and low speed pre-ignition. Knock has been

observed for the first time in 1882 by Sir Dugald Clerk who described it as a “persistent and troublesome enemy” [1] while the first observations of low-speed pre-ignition (LSPI) date back to the beginning of years 2000. However, in both cases, the triggering and the development of the abnormal combustion process rely on the auto-ignition characteristics of the air/fuel mixture.

In order to control these abnormal phenomena, it is necessary not only to better understand how and when an auto-ignition can be triggered by “hot spots”, but also how it will propagate inside the combustion chamber since the auto-ignition intensity and the potential resulting engine damages are linked to both aspects. Different approaches such as the Livengood-Wu integral can be used to predict the auto-ignition temporal onset. However, advanced tools and methodologies are still being developed to better understand and predict the auto-ignition propagation modes.

The original theory regarding the auto-ignition propagation mode was provided by Zeldovich [2] who introduced three main modes by which the reaction front can propagate. The numerical analysis of these modes was then further explored by several groups of researchers, and is still the subject of new investigations. In the early 1990s, mathematical models were introduced for example by Goyal et al. [3] in order to simulate hot spot ignition in one dimensional geometries with H₂-O₂ mixtures and using a detailed mechanism for gas phase reaction. At that time, even mixtures featuring two hot spots could be simulated to study the interactions of two ignition processes as it can be the case in realistic engines conditions. The extension of these works in [4] showed that the transition from deflagration to detonation could also be simulated for CH₄-air mixtures. A dual experimental and numerical analysis was also provided by König et al. [5]. 1D and 2D simulations were performed to take into account burned gases around the hot spot from the very beginning of auto-ignition. The overall theory was further developed by Bradley and co-workers at Leeds University to analyze auto-ignition processes during CAI combustion [6], during knocking combustion [7], and lately during LSPI [8]. Their auto-ignition calculations for 50%H₂-50%CO-air mixtures allowed to highlight and to analyze the different propagation modes in various conditions. A specific classification diagram based on two dimensionless parameters has then been defined. Since then, this so-called “detonation peninsula” has been used for the analysis of both experimental occurrences of auto-ignition [9] and numerical results [10-11]. The recent studies of knocking combustion and LSPI require however to consider fuels whose auto-ignition characteristics are very different from those of H₂-CO. Results obtained with n-heptane-air

and iso-octane-air mixtures have been recently illustrated by Bates et al. [12] but not fully compared to the original results from Gu et al. [13]. More recently, Chen et al. have thoroughly analyzed several simulation results obtained with n-heptane-air mixtures, by considering non-uniform mixture compositions, or even cool spots within the Negative Temperature Coefficient (NTC) region [14]. These results have highlighted the different auto-ignition propagation modes but the characteristics of n-heptane-air mixtures have not been compared to those of H₂-CO-air or TRF-air mixtures, and the detonation peninsula location has not been compared to that defined by Gu et al. [13].

This article aims at confirming the relevancy of the original detonation peninsula when considering realistic fuels used in modern gasoline engines based on similar simulations as those performed by Bradley et al.. The detonation peninsula position has already been discussed during the last Conference on Modeling and Diagnostics for Advanced Engine Systems (COMODIA, Okayama, July 2017) and then published in the International Journal of Engine Research [15] with only an initial condition for P_0 and T_0 . This new study provides further analyses and presents the latest results of the authors.

The first section introduces the main features of the original theory allowing characterizing the auto-ignition propagation mode. The second section introduces the numerical procedure used to reproduce the different auto-ignition propagation modes. The third section focuses then on the main hypothesis involved in the estimation of the key parameters ξ and ε , and shows that final peninsula location strongly depends on this assumption. Finally, different peninsulas are plotted looking at parametric variations as initial conditions in terms of P_0 , T_0 , equivalence ratio and dilution rate.

Theoretical background

Auto-ignition in Spark Ignition (SI) engines appears randomly in time during the engine cycle, after the spark in the case of knocking combustion, or after a first flame propagation phase in the case of LSPI. Regarding its location, auto-ignition is triggered in reactive centers resulting from mixture heterogeneities inside the combustion chamber. These heterogeneities are linked to higher temperatures, to the local mixture composition featuring an increased reactivity (local fuel/air and dilution ratios), or even to external perturbations like solid particles or oil droplets. It is usually assumed, however, that reactive auto-ignition centers correspond to temperature gradients within the mixture that is why these are often called “hot spots”.

Two kinds of waves are generated when auto-ignition is triggered: a reaction wave associated with the chemical propagation of the reactive front and a pressure wave initiated by the thermal explosion of the hot spot at the very beginning of auto-ignition. If the local overpressure generated at the moment of auto-ignition is strong enough to provide a critically short auto-ignition delay time in the surrounding mixture, the reactive front and the pressure wave may couple and form a detonation wave, which propagates throughout the mixture. Both waves are intrinsically linked, since the compression of the mixture close to the hot spot contributes to an increase in reactivity and propagates auto-ignition.

Zeldovich [2] showed that a one-dimensional thermal hot spot characterized by its radius and by its temperature gradient between its center and the surrounding mixture lead to four kinds of auto-ignition propagation modes. The first case corresponds to a supersonic auto-ignition with a reaction wave propagating ahead of the pressure

wave. In Zeldovich’s classification thermal explosions represent a limit case of supersonic auto-ignition with an infinite propagation speed of the reactive front. The second one corresponds to the stationary detonation for which the shock wave compresses the unburned gas ahead of it, thereby supporting and reinforcing the chemical reaction. The pressure and the reaction waves have thus the same speed which is theoretically the Chapman-Jouguet speed. Both waves continuously interact and amplify each other, resulting in high local pressure levels. Finally, the third and the fourth modes concern subsonic auto-ignition propagations, one with the reaction wave faster than the laminar flame speed and the other with the reaction wave slower, so that normal flame propagation driven by the laminar flame speed occurs. The different flame propagation modes issued from auto-ignition are widely discussed in literature [6-14].

This original theory has then been further developed and applied to the analysis of auto-ignition in internal combustion engines by D. Bradley and his co-workers at the University of Leeds [6-8,13]. A specific numerical methodology has been developed to determine the auto-ignition propagation mode around a one-dimensional thermal hot spot characterized by its radius r_0 and by its temperature gradient between its center and the surrounding mixture $\partial T/\partial r$. Two dimensionless parameters (ε, ξ) were defined depending on the hot spot characteristics and on the surrounding fresh gas mixture properties (pressure, temperature, fuel/air equivalence ratio, dilution ratio).

ξ describes the coupling between the acoustic wave propagating at the speed of sound a , and the reaction wave propagation at the speed u_a . It can be written as a dimensionless temperature gradient considering the temperature gradient between the center of the hot spot and the surrounding mixture, and the auto-ignition delay τ_i (Eq. 1).

$$\text{Eq. 1} \quad \xi = \frac{a}{u_a} = \frac{a}{\partial r / \partial \tau_i} = \frac{a}{\partial r / \partial T \cdot \partial T / \partial \tau_i}$$

ξ parameter is also written as a dimensionless temperature gradient by defining a critical hot spot temperature gradient (Eq. 2) for which the chemical resonance between the pressure wave and the reaction front occurs:

$$\text{Eq. 2} \quad \xi = \left(\frac{\partial T}{\partial r} \right) \cdot \left(\frac{\partial T}{\partial r} \right)_c^{-1}$$

with $\left(\frac{\partial T}{\partial r} \right)_c = a^{-1} \cdot \left(\frac{\partial \tau_i}{\partial T} \right)^{-1}$

Theoretically, detonation is achieved as soon as the reaction and pressure waves propagate at the same speed ($\xi = 1$, [16]). However, because of species and thermal diffusion during the induction period, a developing detonation is not stringently restricted to this critical value $\xi = 1$. In fact, depending on the reactivity, a wider range of initial conditions can lead to a developing detonation. Thus, an upper limit ξ_u and a lower limit ξ_l have been introduced to classify the different propagation modes and to define a so-called detonation peninsula.

The second dimensionless parameter ε compares the characteristic chemical time scale given by the excitation time τ_e , and the acoustic time scale given by r_0/a (Eq. 3). By quantifying the rate at which the

auto-ignition chemical energy is released into the acoustic wave, ε measures the hot spot reactivity.

$$\text{Eq. 3} \quad \varepsilon = \frac{r_0/a}{\tau_e}$$

It must be noted that ε and ξ are determined as a function of initial conditions (before chemical reactions start). Usually, characteristics of the fresh gas needed to determine ξ and ε are directly known (pressure, fuel/air ratio) or derived (temperature and dilution) from experimental data or simulations. The main issue is the estimation of the thermal hot spot properties (radius and temperature gradient). In academic cases like 1D simulations of this article, controlling these properties is easy. When considering real engine geometry and conditions, it is much more complex and hot spot properties need to be assumed especially in experiment. The estimation is still difficult using numerical simulations but not impossible looking at distributions of computed gradient and radius for example.

Lots of recent studies [17-20] used this detonation peninsula to analyze experimental and numerical occurrences of knock and LSPI in highly charged SI engines. It is therefore essential to validate the location of this peninsula for realistic gasoline fuel.

Numerical set-up

To analyze auto-ignition behavior, one dimensional calculations are performed using the AVBP compressible and reactive solver co-developed by IFPEN and CERFACS [21]. The computational domain is presented in Figure 1.

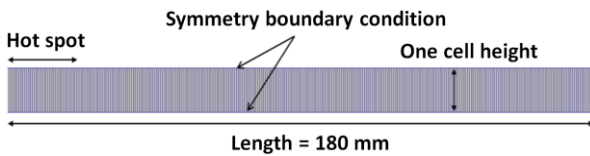


Figure 1: Calculation domain.

A grid convergence has been achieved using cells down to 6 μm and the final mesh used for all calculations owns 3600 cells for a length of 180 mm, which corresponds to cells of 50 μm .

To mimic the hot spot, a linear temperature gradient is initialized on the left part of the domain with a defined amplitude and radius. Figure 2 illustrates this simplified configuration. For this study, T_0 is chosen outside of the Negative Temperature Coefficient (NTC) region where τ_i increases as T decreases.

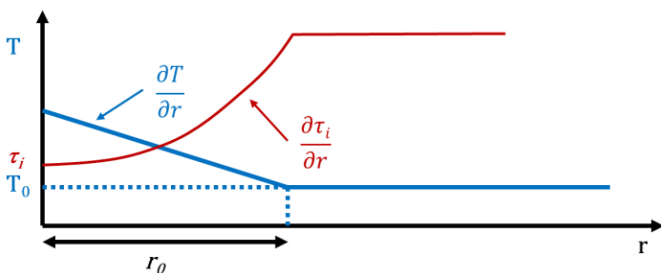


Figure 2: Initial hot spot definition.

A “symmetry“ boundary condition is defined at the center of the hot spot (left part of the domain) and a constant pressure boundary condition is defined at the outlet.

Regarding initial conditions, the domain is fueled using an air-TRF mixture (RON95 surrogate with 42.8% isooctane, 13.7% n-heptane, 43.5% toluene). Different thermodynamic conditions in terms of pressure P_0 and temperature T_0 in the homogeneous part of the domain are analyzed to be as close as possible to real engine conditions. However, the NTC region that is usually obtained below 900 K is not investigated in this article as it needs the use of a “cold spot” and not a “hot spot”, but will be part of future studies. Variations of equivalence ratio and EGR rate are also analyzed in the result part of the article (these two last parameters being considered in the framework of lean and diluted SI engines).

Involving a complex chemical mechanism in numerical codes to solve chemistry of realistic fuels requires computing thousands of species and reactions. This methodology is too CPU time consuming as the objective is to analyze a large number of operating conditions to precisely define the detonation peninsula. The tabulated model TKI-LES model [15-22] has thus been chosen to simulate auto-ignition as previous studies have already shown its ability to catch such phenomenon [23]. This model is based on a look-up table of τ_i and τ_e , obtained using a priori calculations for the same surrogate fuel in homogeneous reactors and considering the LLNL kinetic mechanism with 1388 species and 5935 reactions [24]. The chemical computations are first performed with an in-house code named CLOE (based on the Senkin solver), and the resulting auto-ignition characteristic time scales (τ_i, τ_e) are then tabulated for different pressure, temperature, EGR and equivalence ratio levels. The auto-ignition delay time τ_i is defined as the time needed to increase the mixture temperature by 400 K compared to the initial conditions. The excitation time τ_e is the time required for the heat release rate to rise from 5% to its maximal value. This characteristic time being of the order of μs , a high temporal resolution is required for the post-processing to guarantee accurate calculations. The values of τ_i and τ_e are just read in the table during the 1D calculations.

Calculation hypothesis for ε and ξ

The reactivity and coupling parameters (ε, ξ) are defined using the initial conditions of the domain. Referring to the original works of Gu and Bradley, the initial temperature at $r = r_0/2$ is used to determine τ_i and τ_e , then to calculate ε and ξ . The choice of the reference temperature location has a significant impact on the calculation of (ε, ξ) values. This topic has already been discussed in [15] but Figure 3 shows for other initial conditions, the variations of these parameters as a function of the temperature increase at the center of the hot spot ΔT_0 for three hypotheses: when the reference temperature is taken at the outer limit of the hot spot (assumption n°1, $r = r_0$), at the middle of the hot spot (assumption n°2, $r = r_0/2$), and at the center of the hot spot (assumption n°3, $r = 0$).

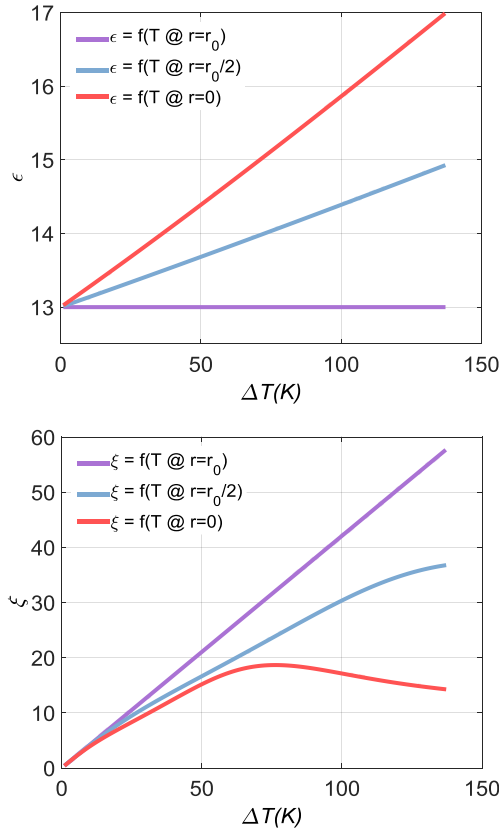


Figure 3: Impact of the reference temperature on ε (top) and ξ (bottom) values as a function of ΔT_0 at the center of the hot spot ($r_0 = 29.6$ mm, $P_0 = 50$ bar, $T_0 = 900$ K, $\phi = 1$, no dilution).

Even if thermal initial conditions are really different, conclusions are the same as in [15]. For the highest ΔT_0 , the estimation of the two parameters varies a lot, meaning that for the same initial conditions, the position on the detonation peninsula is totally different. Table 1 summarizes the ε and ξ values obtained by considering these three different assumptions for the same hot spot configuration ($r_0 = 29.6$ mm and $\Delta T_0 = 100$ K). The impact of the reference temperature on ε is rather limited but the impact on ξ values is really significant. Of course, only one single auto-ignition propagation mode (a subsonic deflagration) is obtained for this hot spot configuration as initial conditions are the same, but the chosen assumption has a large impact on peninsula limit position.

For the fuel sensitivity analysis conducted in this study, a proper comparison with the original detonation peninsula provided by Gu and Bradley can only be achieved if a similar assumption is made regarding the choice of the reference temperature. The estimation of (ε , ξ) at $r = r_0/2$ is used for the following cases.

Table 1: Impact of the reference temperature on (ε , ξ) values for $\Delta T_0 = 100$ K ($r_0 = 29.6$ mm, $P_0 = 50$ bar, $T_0 = 900$ K, $\phi = 1$, no dilution).

Assumption	ε	ξ
1: T @ $r = r_0$	13.0	17.6
2: T @ $r = r_0/2$	14.3	30.2
3: T @ $r = 0$	15.9	41.8

Figure 3 also shows that the variation of ξ with ΔT_0 is not monotonic. For the example considered, ξ reaches a maximal value around 19 for ΔT_0 close to 70 K and then slightly decreases. This particular behavior is observed with TRF-air mixtures because their critical temperature gradient is increasing (as ΔT_0 increases) faster than the temperature gradient (Eq. 2) around the hot spot. This behavior is related to the specific auto-ignition delay variation as a function of the temperature for TRF-air mixtures and was not reported so far in the case of H₂-CO-air mixtures because the maximal ξ value for these mixtures is much higher (around 100 for the same initial conditions as Figure 3 of [15]).

Results

Auto-ignition mode classification

Hundreds of calculations have been performed with multiple initial conditions regarding the hot spot and the surrounding mixture. An automatic post-processing procedure has been defined to quickly identify the auto-ignition propagation mode for each considered case. This post-processing procedure is based upon the analysis of the relative position and velocity of the reaction and pressure waves. The analysis is carried out at the moment when the reaction wave reaches $r = r_0$, just before the reaction begins its propagation into a perfectly homogeneous mixture.

Theoretically, the detonation mode is reached when the positions and speeds of the reaction and pressure fronts perfectly coincide. However, a tolerance of 10% is used here on speed and position in order to take into account transition phenomena during which pressure and reaction fronts chase each other. The criteria used to differentiate the main modes of propagation are summarized in Table 2 as a function of the reaction and pressure wave speeds and positions (respectively named u_a , x_a , a , x_p).

Table 2. Identification criteria for auto-ignition propagation modes.

	Reaction front speed	Reaction front position
	u_a	x_a
Developing detonation	$0.9*a < u_a < 1.1*a$	$0.9*x_p < x_a < 1.1*x_p$
Subsonic deflagration	$u_a \leq 0.9*a$	$x_a \leq 0.9*x_p$
Supersonic deflagration	$u_a \geq 1.1*a$	$x_a \geq 1.1*x_p$

Thanks to these criteria, the automation of the data post-processing made possible to build several peninsulas for various conditions in terms of pressure, temperature, equivalence ratio and dilution rate. These new detonation peninsulas are presented in the next section.

Detonation peninsulas

Figures 4 to 6 show the three detonation peninsulas obtained for initial temperature T_0 varying between 900 and 1100 K.

The maximal temperature at the center of the hot spot depends on its radius and temperature gradient. In order to analyze auto-ignition events occurring in realistic engine conditions, it is therefore necessary to confront the assumptions made for the hot spot with realistic mixture characteristics in engines and especially with the maximal fresh gases temperature. For this reason, the maximal temperature assumed at the center of the hot spot cannot exceed 1200 K, which is already a very high temperature in engine operating

conditions. For given hot spot radius r_0 and initial temperature T_0 , the maximal temperature gradient around the hot spot is thus limited. Consequently, the maximal attainable ξ value is also limited. This limitation is shown by the blue areas in Figures 4 to 6, pointing out that the area of the relevant domain depends on the level of temperature T_0 . The higher T_0 is, the lower maximal value for ξ are, because large hot spot radii with high temperature gradients (high values of ξ) would lead to non-realistic temperature at the center of the hot spot. It can also be noticed in Figure 6 that the upper limit of the new peninsula (red dotted line) is shortened at $\varepsilon \approx 10$ as it crosses the upper limit of the relevant engine region.

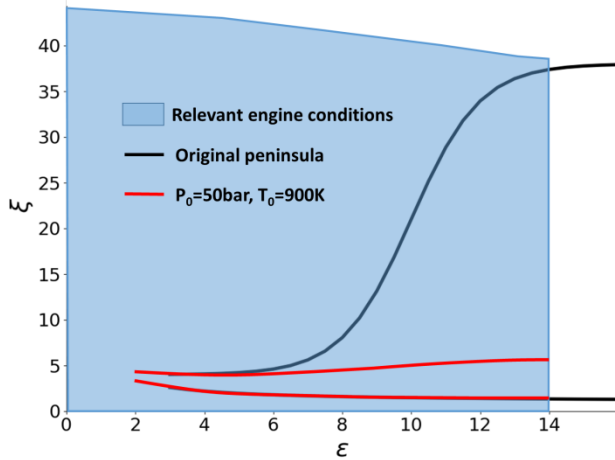


Figure 4: Computed detonation peninsula with $T_0 = 900$ K ($P_0 = 50$ bar, $\phi = 1$ and EGR = 0%).

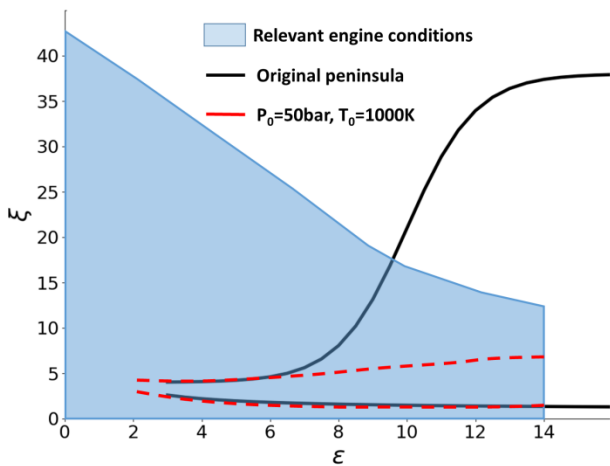


Figure 5: Computed detonation peninsula with $T_0 = 1000$ K ($P_0 = 50$ bar, $\phi = 1$ and EGR = 0%).

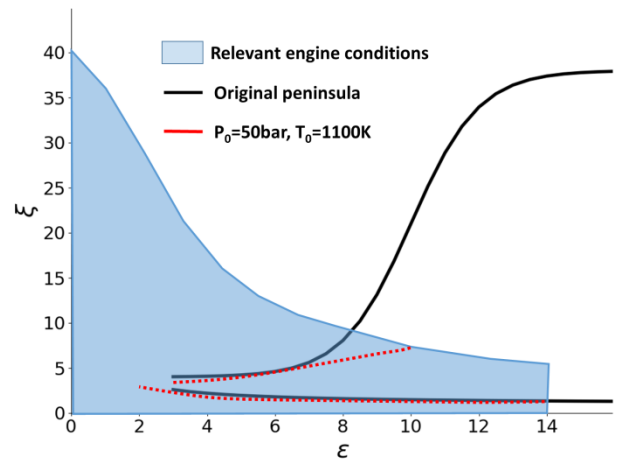


Figure 6: Computed detonation peninsula with $T_0 = 1100$ K ($P_0 = 50$ bar, $\phi = 1$ and EGR = 0%).

The hot spot radius has also been limited to a few millimeters in order to represent typical mixture heterogeneities in SI engines. However, in some specific cases (when auto-ignition occurs early during the cycle for example), the premixed flame front is still in the middle of the combustion chamber. The available fresh gases length is not the distance between flame front and the liner, but the circumference of the combustion chamber, allowing potentially larger hot spots. The authors considered thus that hot spot radius around 20 mm are still acceptable even if in a real engine, the probability to obtain in such huge hot spot radii is low.

Defining a maximal hot spot radius r_0 value directly implies a maximal value of the reactivity parameter for engine cases at a given pressure and temperature. Figure 7 shows the evolution of r_0 depending on parameter ε for three initial temperatures T_0 . When the temperature increases, excitation time decreases and based on Eq. 3, the ε value increases if the sound speed variation is neglected. However, the initial temperature T_0 has a limited influence on the evolution of r_0 at a given ε value. If realistic hot spot radii (lower than 20 mm) are considered, region where ε is higher than 10 should not be reached when analyzing auto-ignition events in SI engines. In order to extend the analysis, values of ε until 14 are studied in this paper, upper limit which is still lower than the original peninsula one.

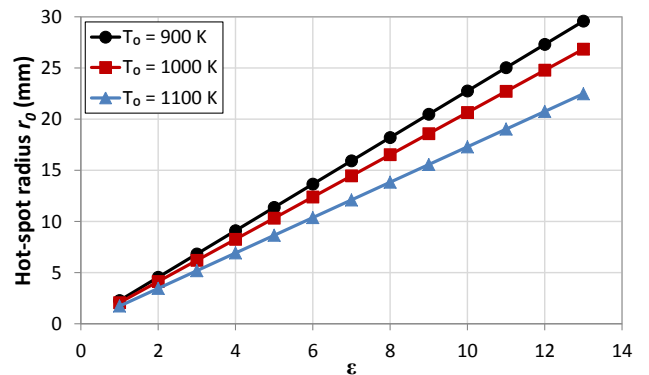


Figure 7: Evolution of the hot spot radius r_0 as a function of ε for three different initial temperatures T_0 ($P_0 = 50$ bar, $\phi = 1$ and EGR = 0%).

Focusing now on the new detonation peninsula locations predicted by numerical calculations (red lines), results from Figures 4 to 6 are

presented on the same graph in Figure 8 (using a logarithmic scale for the ξ axis to improve readability). Whatever the initial temperature chosen, new detonation peninsulas have a close location. However, the upper limit of the detonation peninsula estimated in this study is lower than the original one for values of the reactivity parameter ε between 8 and 14, reducing the region where detonation can occur.

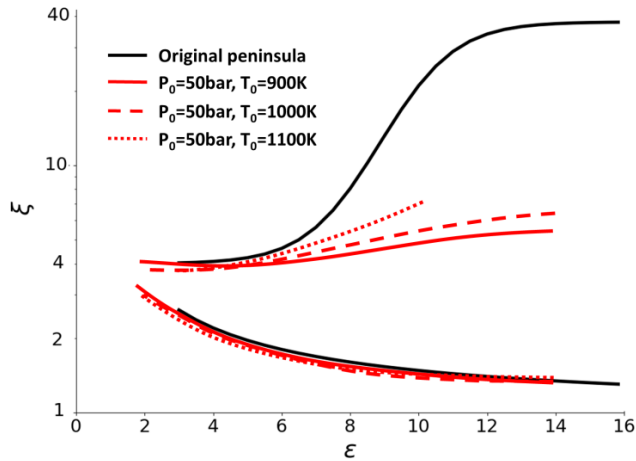


Figure 8: Computed detonation peninsulas with $P_0 = 50$ bar, $\phi = 1$, EGR = 0% and for three initial temperatures T_0 .

A variation of the pressure P_0 is also achieved with initial levels of 40, 50 and 70 bar. The resulting detonation peninsulas are presented in Figure 9 (red lines) in comparison to the original one. The relevant engine domain is not presented here but is quite similar to the one shown in Figure 5 as it depends little on the initial value of P_0 . The evolution of the hot spot radius over ε is also not presented here as the impact of P_0 is still much more limited than the influence of T_0 . Looking at the position of the three new peninsulas, the small difference induced by the pressure change can be neglected. A slight vertical shift is observed but clear borders are impossible to establish precisely (as a reminder, arbitrary margins of 10% are used to detect detonation), that is why new detonation peninsulas are considered to be consistent with the original peninsula except for the upper limit where ε is greater than 8). As for the T_0 variation, the predicted peninsulas are much thinner, reducing thus a lot the probability to observe a developing detonation.

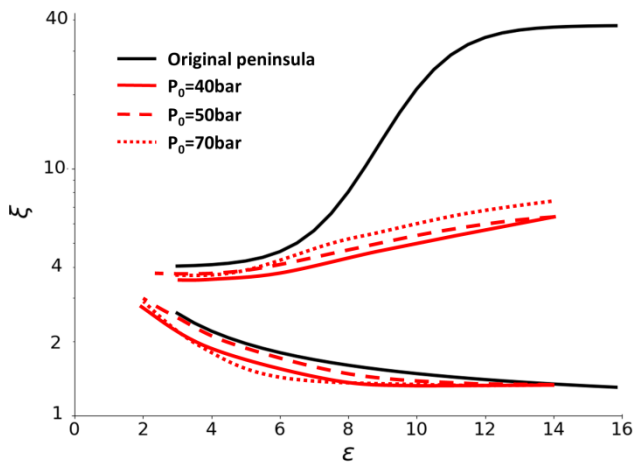


Figure 9: Computed detonation peninsulas with P_0 between 40-70 bar ($T_0 = 1000$ K, $\phi = 1$ and EGR = 0%).

The variation of initial equivalence ratio (see Figure 10) points out that the upper limit of the new peninsulas is moving down as the equivalence ratio is increasing. This evolution is limited but the overall surfaces of the new peninsulas are lower than the original one for values of ε higher than 8, as for the two previous parametric variations.

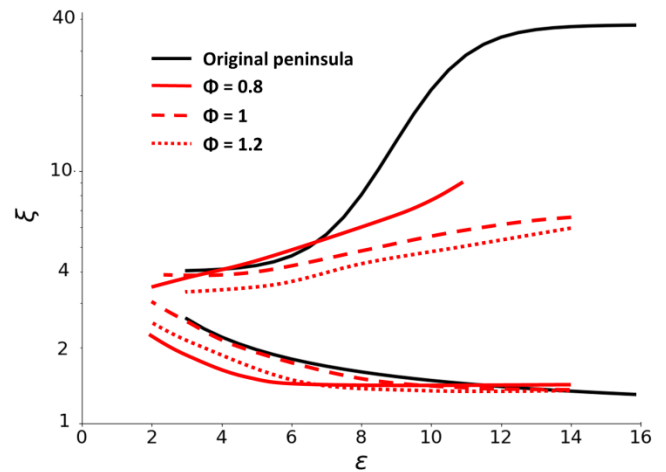


Figure 10: Computed detonation peninsulas with ϕ varying between 0.8 and 1.2 ($P_0 = 50$ bar, $T_0 = 1000$ K and EGR = 0%).

Figure 11 shows that much higher hot spot radii are required with lean mixtures to reach similar reactivity parameter ε as for stoichiometric mixtures. Indeed, when the fuel-air equivalence ratio is decreased, the excitation times are also significantly decreased which explains that the reactivity parameter is lower in lean conditions than in stoichiometric conditions for a given hot spot radius. It must be noted, however, that these fuel-air equivalence ratio variation has been performed with constant pressure and temperature which would not be possible in an engine.

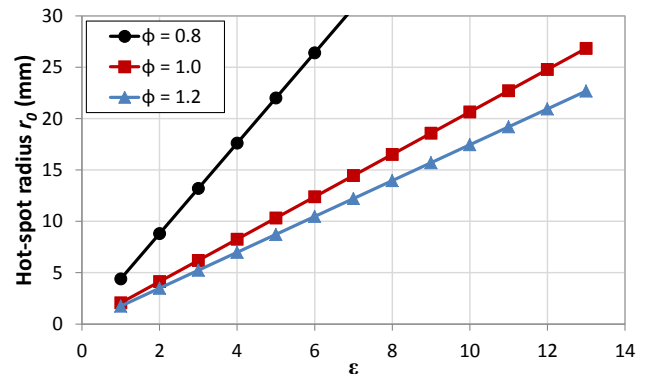


Figure 11: Evolution of the hot spot radius r_0 as a function of ε for three different initial equivalence ratios ($P_0 = 50$ bar, $T_0 = 1000$ K and EGR = 0%).

The last parametric variation of the initial conditions is the dilution rate. In this study, the real composition of exhaust gases is not considered and the dilution is performed with pure nitrogen only (called EGR in the following figures). The dilution rate was varied between 10 and 30% in volume. It is important to notice that the initial temperature T_0 is kept constant to 1000 K for these investigations, whereas the main objective of dilutant addition at high load in SI engines is to reduce end gases temperature.

Figure 12 points out the large effect of the dilution rate on the calculation of the reactivity parameter ε at a given hot spot radius r_0 . Indeed, the excitation time sharply increases when dilution rate increases, which reduces the maximal attainable value of ε to keep initial radius r_0 consistent with mixture heterogeneities length scale in SI engines. In other words, for high dilution rates, the developing detonation peninsula is very thin and should be limited to a maximum value of $\varepsilon = 2$.

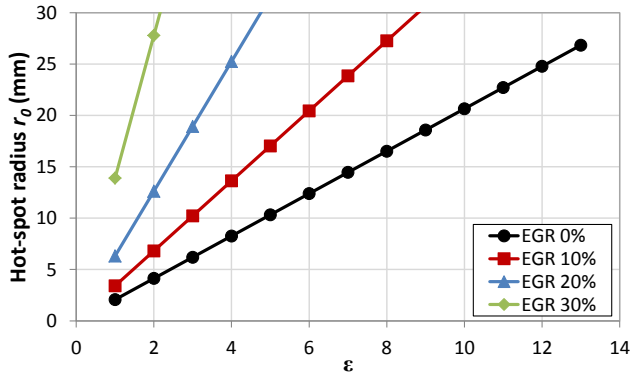


Figure 12: Evolution of the hot spot radius r_0 as a function of ε for four different initial dilution rates ($P_0 = 50$ bar, $T_0 = 1000$ K, and $\phi = 1$).

However, the new peninsulas presented in Figure 13 do not take into account this aspect in order to provide a fuller comparison of the considered configurations. For this new variation, the impact is much more visible: the detonation peninsula clearly moves from right to left and the upper limit of the detonation peninsula is much steeper when dilution rate increases.

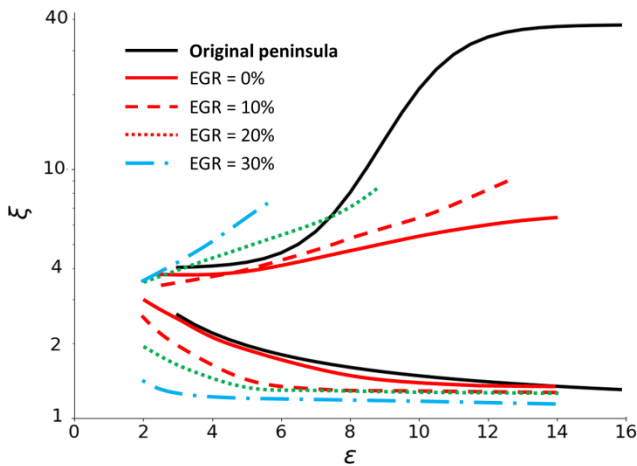


Figure 13: Computed detonation peninsulas with EGR rates varying between 0 and 30% ($P_0 = 50$ bar, $T_0 = 1000$ K and $\phi = 1$). A logarithmic scale is used for ξ .

Summary

The location of the detonation peninsula has been studied as a function of the hot spot characteristics, and as a function of four parameters characterizing the surrounding mixture: the initial temperature and pressure, the fuel-air equivalence ratio and the dilution rate.

In all cases, the new detonation peninsulas obtained for TRF-air mixtures are much thinner than the original one defined for H_2 -CO-air mixtures, especially for ε values higher than 8.

On one hand, the initial temperature and pressure (T_0 and P_0) around the hot spot only have a very limited impact on the upper and lower limits of the detonation peninsula.

On the other hand, the fuel-air equivalence ratio and the dilution rate have a much stronger effect on the detonation peninsula, and particularly on the position of its upper limit. Diluting the mixture with air or with EGR leads to significant increases in excitation times τ_e , and consequently only very low ε values can be reached with realistic hot spot radii. Besides, the upper limit of the detonation peninsula is getting steeper and steeper at low ε values when the dilution rate increases.

Conclusions

This article aims at verifying the developing detonation peninsula location for a TRF fuel compared to the original one proposed by Bradley and his coworkers for H_2 -CO.

1D calculations have been performed for various (ε , ξ) values corresponding to real engine operating conditions. This analysis is based on the assumption that hot spots in real engine conditions cannot exceed around 20 mm of radius, and that their maximal temperature is lower than 1200 K. It is also important to keep in mind that the resulting locations for detonation peninsulas depends on the used classification criteria, chosen here at $r = r_0/2$. It follows a possible SI engine zone located between 0 and 10 for the reactivity parameter ε (extended to 14 in this study) and between 0 and 45 for coupling parameter ξ .

An automatic post-processing method has been developed and validated to analyze the hundreds of 1D calculations needed for each peninsulas. This methodology makes possible the achievement of variations of initial pressure, temperature, fuel-air equivalence ratio or dilution rate.

The analysis of detonation peninsulas points out that the location of the developing detonation zone is independent of the initial pressure or temperature level. Its location is more affected by the increase of the equivalence ratio (which tends to make thinner the developing detonation zone) and much more by the dilution rate which is responsible for an increase of the area of the detonation peninsula at low ε values. Finally, based on all the studied cases, it can be stated that the original detonation peninsula obtained for H_2 -CO mixture is also valid for TRF fuel at ε values lower than 8, but overestimates the developing detonation region for ε between 8 and 14.

The use of the detonation peninsula to analyze auto-ignition intensity is not limited to abnormal combustion. This tool can also be used to better understand advanced combustion concepts such as Spark Assisted Compression Ignition (SACI) for which auto-ignition must be controlled, but not avoided, to increase the efficiency without damaging the engine. Indeed, the evolution of ε points out that the lean mixture and dilution rate up to 30% reduces the detonation peninsula to a very thin zone. An easier control of SACI combustions seem to be directly linked to longer fuel excitation time, combined with the use a lean or diluted mixture.

In future works, the choice of initial temperature T_0 in the NTC region, using “cold spots” will be investigated to complement this study. The influence of dilution rate at lower initial temperatures has also to be analyzed, as one of the more important effect of dilution is the cooling of fresh gases. The next step will then be to combine these new detonation peninsulas obtained with diluted TRF-air mixtures with 3D calculations in order to maximize the controllable auto-ignition fraction during combustion and thus the efficiency.

References

1. Clerk, D., Transactions of the Faraday Society 22 (1926), 338-340.
2. Zeldovich, Y.B., Combust. Flame 39 (1980) 211-214.
3. Goyal, G., Maas, U., Warnatz, J., SAE Technical Paper 900026, 1990.
4. Goyal, G., Warnatz, J., Maas, U., Proc. Combust. Inst., 23 (1991) 1767-1773.
5. König, G., Maly, R., Bradley, D., Lau, A., Sheppard, C., SAE Technical Paper 902136, 1990.
6. Bradley, D., Morley, C., Emerson, D.R., SAE Technical Paper 2002-01-2868, 2002.
7. Bradley, D., Morley, C., Walmsley, H. L., SAE Technical Paper 2004-01-1970, 2004.
8. Kalghatgi, G.T., Bradley, D., Int. J. Engine Res. 13 (2012), 399-414.
9. Rudloff, J., Zaccardi, J-M., Richard, S., Anderlohr, J.M., Proc. Combust. Inst. 34 (2013) 2959-2967.
10. Robert, A., Richard, S., Colin, O., Poinot, T., Comb. and Flame 162 (2015) 2788-2807.
11. Misdariis, A., Vermorel, O., Poinot, T., Proc. Combust. Inst. 35 (2015) 3001-3008.
12. Bates, L., Bradley, D., Paczko, G., Peters, N., Comb. and Flame 166 (2016), 80-85.
13. Gu, X.J., Emerson, D.R., Bradley, D., Combust. Flame 133 (2003) 63-74.
14. Dai, P., Chen, Z., Chen, S., Ju, Y., Proc. Combust. Inst. 35 (2015) 3045-3052
15. Robert A., Zaccardi J-M, Dul C., Guerouani A., Rudloff J., Int. J. Engine Res., (2018) , published on-line.
16. Zeldovich, Y.B., Librovich, V.B., Makhviladze, G.M., Sivashinsky, G.I., Astronaut. Acta 15 (1970) 313-321.
17. Peters N, Kerschgens B, Jochim B and Paczko G. Proc. of the 4th Int. Conf. on knocking in gasoline engines, (2013) Berlin
18. Tanoue et al., Int. J. Engine Res., 17 (2016) , 666-676
19. Netzer, C., Seidel, L., Pasternak, et al., SAE Technical Paper, 2017-01-0538, 2017.
20. Bates, L. and Bradley, D, Combust. Flame 175 (2017) 118-122
21. Gourdain, N., Gicquel, L., Staffelbach, G., Vermorel, O., Duchaine, F., Bousuge, J.-F., Poinot, T., Comput. Sci. Discovery 2(1) (2009) 015004.
22. Colin, O., Da Cruz, A. P., Jay, S., Proc. Combust. Inst. 30 (2005), 2649-2656.

23. Robert, A., Richard, S., Colin, O., Martinez, L., De Francqueville, L., Proc. Combust. Inst. 35 (2015), 2941-2948.
24. Mehl, M., Pitz, W. J., Westbrook, C. K. and Curran, H. J., Proc. Combust. Inst. 33 (1) (2011) 193-200.

Contact Information

Dr. Anthony ROBERT, anthony.robert@ifpen.fr

Dr. Jean-Marc ZACCARDI, j-marc.zaccardi@ifpen.fr

IFP Energies nouvelles, Institut Carnot IFPEN TE., 1-4 Avenue du Bois Préau, 92852 Rueil-Malmaison, France

Definitions/Abbreviations

τ_i	Auto-ignition delay time
τ_e	Excitation time
ε	Hot spot reactivity
ξ	Coupling parameter
$\partial T / \partial r$	Hot spot temperature gradient
$(\partial T / \partial r)_c$	Critical hot spot temperature gradient
a	Acoustic speed
r_0	Initial hot spot radius
ΔT_0	Temperature increase at the hot spot
P_0	Initial pressure outside the hot spot
T_0	Initial temperature outside the hot spot
ϕ	Fuel-air equivalence ratio
u_a	Reaction wave speed
x_a	Reaction wave position
x_p	Pressure wave position